Supplement of Atmos. Meas. Tech., 18, 5415–5434, 2025 https://doi.org/10.5194/amt-18-5415-2025-supplement © Author(s) 2025. CC BY 4.0 License.





Supplement of

Above Cloud Aerosol Detection and Retrieval from Multi-Angular Polarimetric Satellite Measurements in a Neural Network Ensemble Approach

Zihao Yuan et al.

Correspondence to: Zihao Yuan (z.yuan@sron.nl)

The copyright of individual parts of the supplement might differ from the article licence.

Table S1. Input, output, and training settings of the three NNs.

NN type	Cloud mask	ACA retrieval	Forward model part 1	Forward model part 2	
Input	Radiance, DoLP, scattering angle, SZA, VZA, RAA		state vector of fine mode aerosol ¹ , dust mode aerosol ² and liquid clouds ³ , scattering angle, SZA, VZA, RAA		
Output	Liquid cloud fraction & ice cloud fraction	Total ACAOT (440, 550 and 670 nm), AE (440-670 nm)*, SSA (550 nm), state vector of fine mode aerosol ¹ , dust mode aerosol ² and liquid clouds ³	Radiance	DoLP	
Number of ensembles	3	16	6		
Number of layers	5 (3 hidden layers)				
Number of neurons per layer	64	128	192		
Total size of training set	8 million	16 million	16 million		

¹State vector of fine mode: ACAOT at 550 nm, ALH, effective radius, effective variance, refractive index (real part of inorganic, imaginary part of black carbon and imaginary part of organic carbon)

²State vector of dust mode: ACAOT at 550 nm, ALH, effective radius, effective variance, refractive index (imaginary part of dust)

³State vector of liquid clouds: COT, CTH (cloud top height), CER (cloud effective radius), CEV (cloud effective variance)

^{*}The AE in the paper is calculated from ACAOT at 440 and 670 nm. The AE from NNs direct output is not used in the paper

Table S2. RMSE, MAE and bias of ACAOT_550, AE_440-670 and SSA_550 on synthetic experiments.

RMSE	ACAOT 550	AE 440-670	SSA 550
general	0.107	0.418	0.046
Fine-mode dominated	0.109	0.552	0.052
Dust-mode dominated	0.117	0.403	0.031
MAE	ACAOT 550	AE 440-670	SSA 550
general	0.069	0.313	0.029
Fine-mode dominated	0.071	0.416	0.033
Dust-mode dominated	0.074	0.311	0.022
Bias	ACAOT 550	AE 440-670	SSA 550
general	0.007	-0.010	0.011
Fine-mode dominated	0.018	-0.388	0.016
Dust-mode dominated	-0.015	0.271	0.002

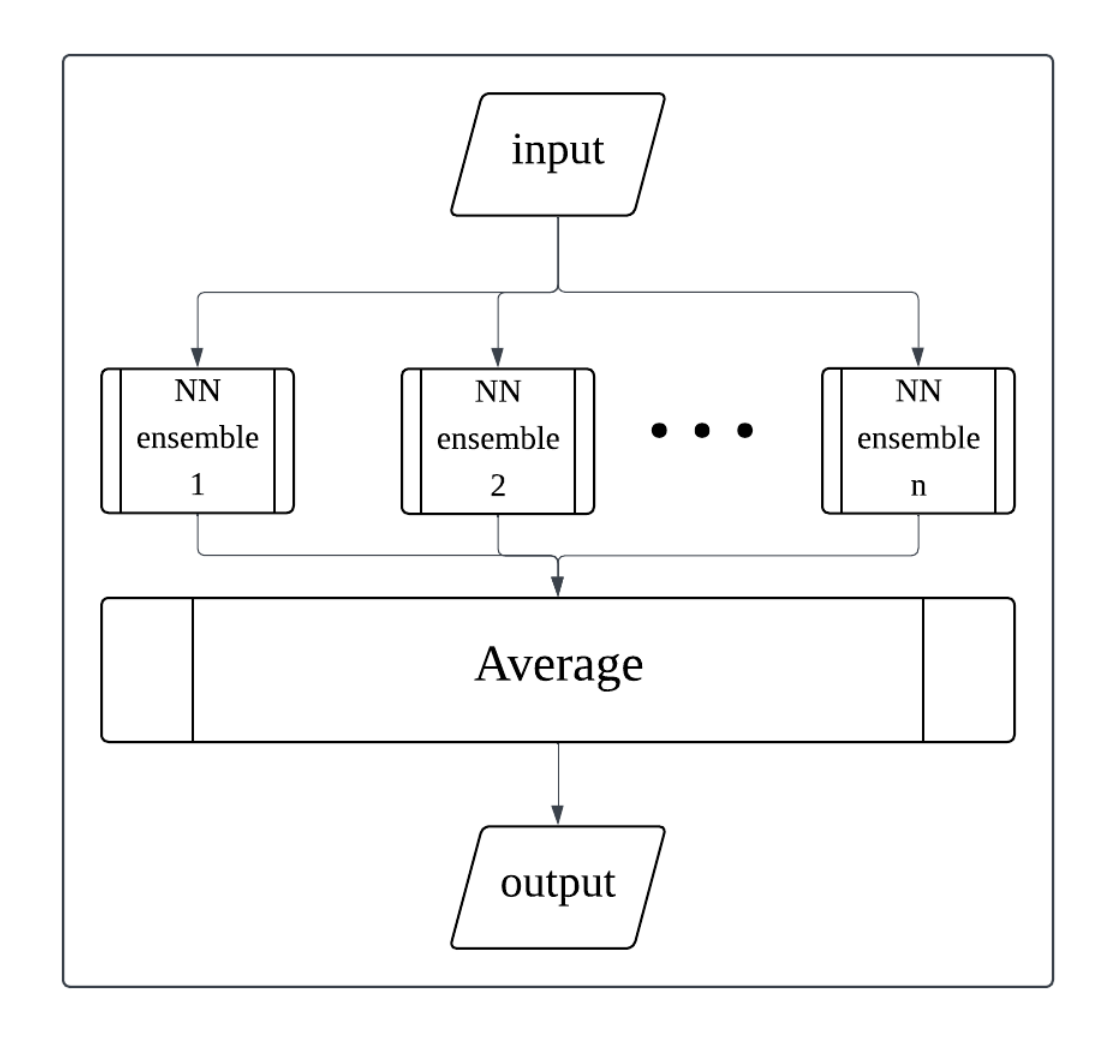


Fig S1. Demonstration of NN ensemble approach used in this paper.

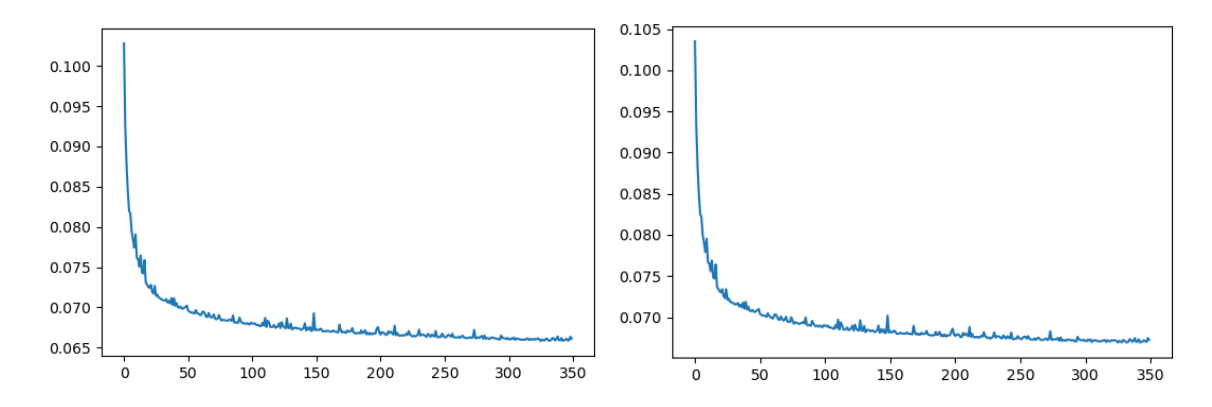


Fig S2. Loss function v.s training epoch on training set (left) and holdout set (right) for ACA retrieval NN, ensemble 1.

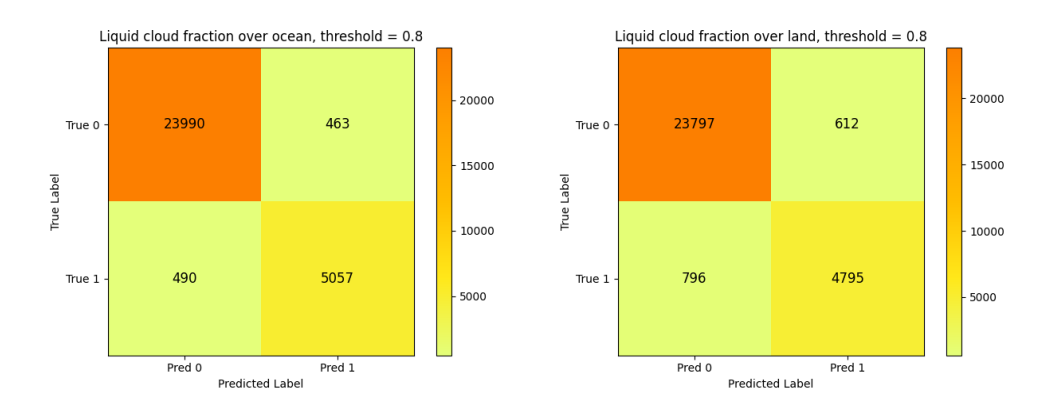


Fig S3. Confusion matrix of liquid cloud detection on the holdout set, "pred 1" means predicted liquid cloud fraction > 0.8, "true 1" means true liquid cloud fraction > 0.8.

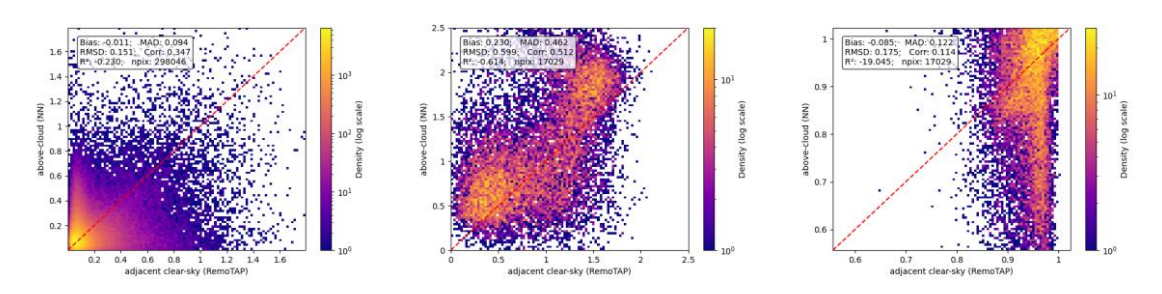


Fig S4. NN ACA retrievals v.s. adjacent PARASOL-RemoTAP clear sky retrievals. No goodness-of-fit mask applied. Other filters are the same as in section 5.1 of the paper.

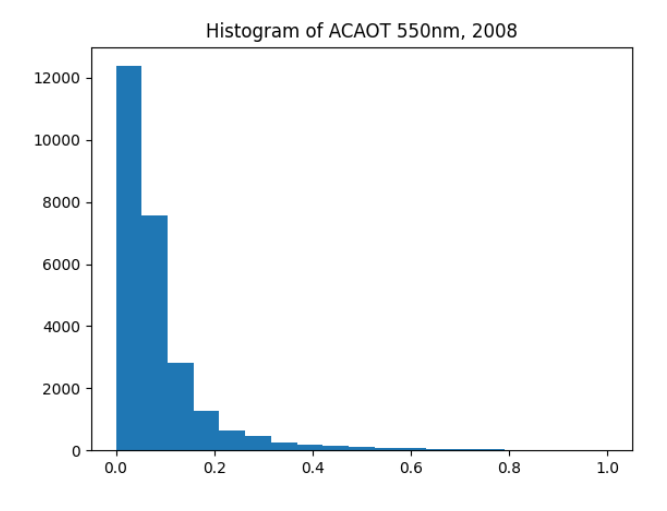


Fig S5. Histogram of ACAOT (550nm) for the whole year 2008 PARASOL-NN ACA retrievals.

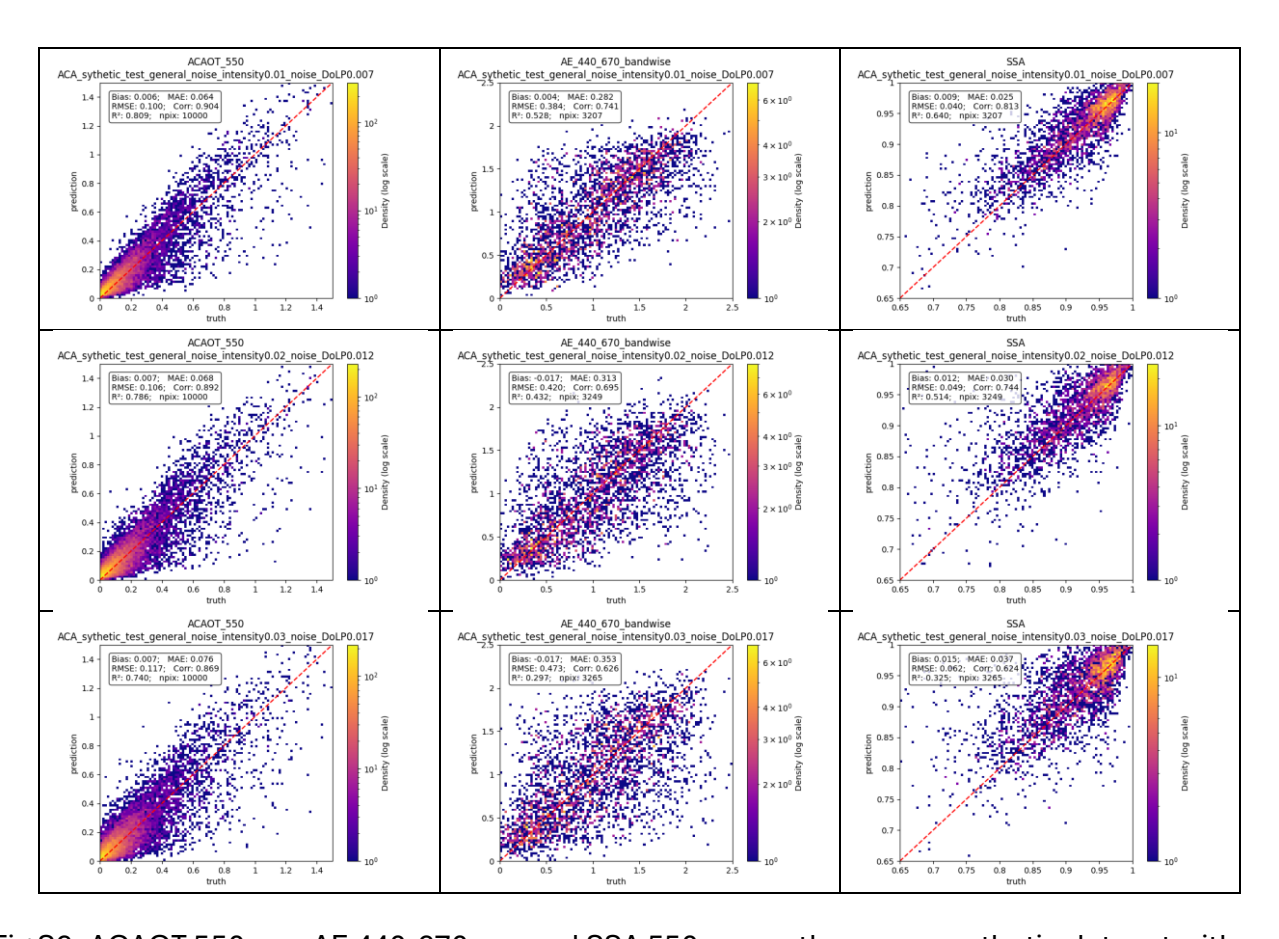


Fig S6. ACAOT 550 nm, AE 440-670 nm and SSA 550 nm on the same synthetic dataset with different noise levels. The first line's noise settings are 1% to intensity and 0.007 to DoLP. The second line is 2% to intensity and 0.012 to DoLP. The third line is 3% to intensity and 0.017 to DoLP.

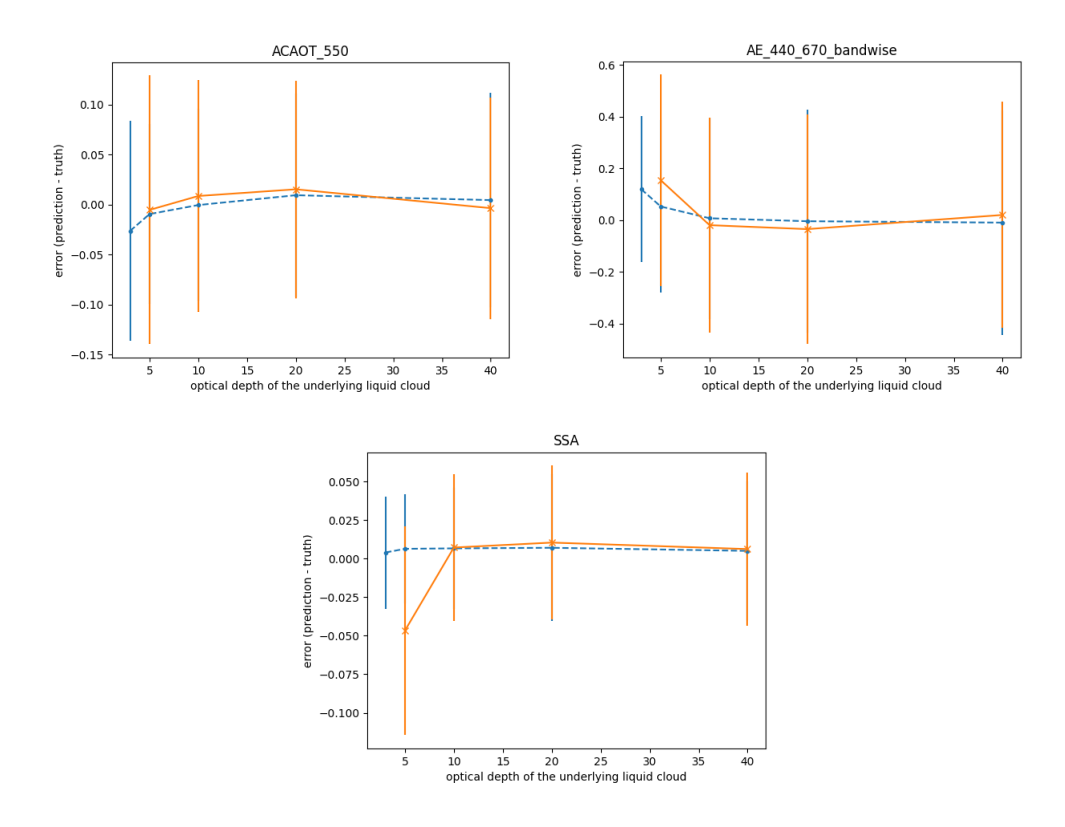


Fig S7. Error and standard deviation of ACAOT, AE and SSA retrievals in different COT bins. Blue lines are over ocean and orange lines are over land.

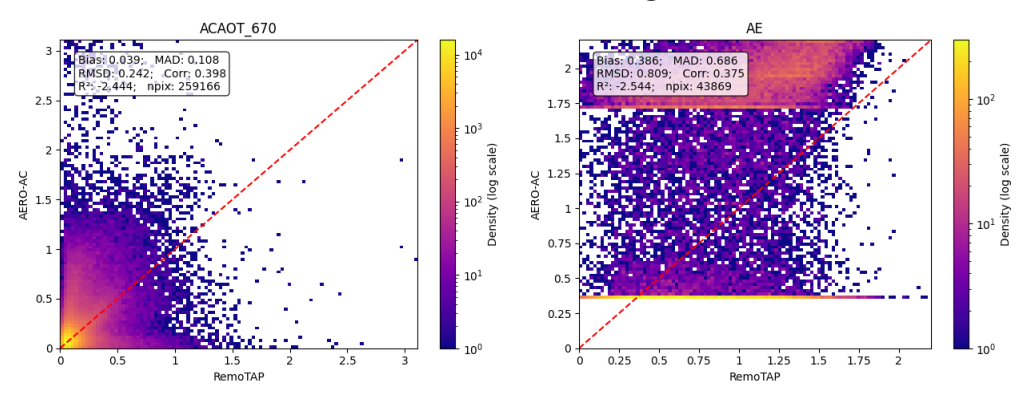


Fig S8. Comparison of ACAOT at 670 nm and AE between PARASOL-RemoTAP clear-sky aerosol retrievals and AERO-AC above cloud aerosol retrievals. Note that the AE from PARASOL-RemoTAP is between 440 nm and 670 nm while that from AERO-AC is between 67 nm and 865 nm.

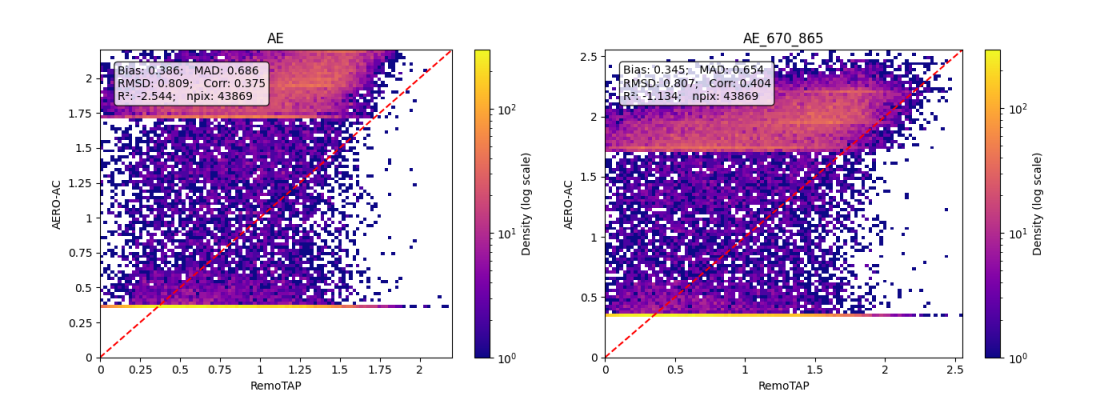


Fig S9. AE Difference in wavelength pair selection. The left panel shows comparison between AERO-AC AE (670-865) with adjacent PARASOL-RemoTAP clear sky AE (440-670), and the right panel shows comparison between AERO-AC AE (670-865) with adjacent PARASOL-RemoTAP clear sky AE (670-865).